04

Spectral and diffraction properties of holographic photopolymer materials with photoinitiating systems based on a charge transfer complex and a coinitiator

© D.I. Derevyanko[1,2], V.V. Shelkovnikov[1,3], E.F. Pen[2,3], S.I. Aliev[1], V.V. Bardin[1], A.D. Bukhtoyarova[1]

[1] Novosibirsk Institute of Organic Chemistry named after N.N. Vorozhtsov SB, Russian Academy of Sciences
Novosibirsk, Russia
[2] Institute of Automation and Electrometry, SB, Russian Academy of Sciences,
Russia, Novosibirsk, Russia
[3] Novosibirsk State Technical University,
Novosibirsk, Russia

e-mail: derevyanko@nioch.nsc.ru

Received May 03, 2024
Revised September 17, 2024
Accepted September 17, 2024

(*Photoinitiating systems*, (PIS)) have been developed based on a photosensitive (*Charge Transfer Complex*, CTC), butyltris(4-anisyl)borate diethyl-9-oxo-10-(4-heptyloxyphenyl)-9H-thioxanthenonium, and a dye-coinitiator, Methylene Blue (MB) with butyltris(4-anisyl)borate tetrabutylammonium. Spectral properties and sensitivity of photopolymer materials based on individual and combined PIS (CTC, MB,CTC-MB) in the holographic recording mode have been studied. It has been shown that PIS-MB andPIS-CTC have sensitivity in a wide spectral range (400−700 nm). Using laser radiation with wavelengths $\lambda_1 = 457$ nm, $\lambda_2 = 532$ nm and $\lambda_3 = 639$ nm, monochrome and color reflection holograms with high diffraction efficiency (50−90%) were formed. Prevention of oxygen inhibition of radical polymerization in 30 μm thick layers of photopolymer materials was experimentally confirmed using butyltris(4-anisyl)borate tetrabutylammonium as a donor component in CTC and as a co-initiator in MB. Modulation of the refractive index during hologram recording, both with and without a protective film preventing oxygen access, was $\Delta n \approx 0.008$.

Keywords: photoinitiating systems, charge transfer complexes, photopolymer materials, reflection holograms.

DOI: 10.61011/EOS.2025.01.60564.6562-24

Introduction

The (*holographic photopolymer materials*, HPPM) are well-known and widely used in the sphere of security holography, optical memory, displays and sensors due to their characteristics and user-friendliness [1–7].

Along with this, the mechanisms of holographic recording and modification of this type of materials are still under study [8–13]. Major components of HPPM include a polymer binder, monomer and photo-initiating system [14–16]. Important characteristics of PIS are the spectral sensitivity range, effectiveness of polymerization initiation, and ability to discolor the sensitizer dye [17].

In case of color holograms the HPPM shall have spectral sensitivity in the wide range of visible spectrum 400−700 nm and a recording energy within 30−70 mJ/cm^2 [18–23]. One of the approaches to provide sensitization of radical polymerization is the use of photosensitive Charge Transfer Complexes (CTC) [24,25]. The CTC formation mechanism can be described qualitatively as the result of an electron transfer from the highest occupied molecular orbital (HOMO) of a donor to the lowest unoccupied molecular orbital (LUMO) of an acceptor. Such PIS are featuring the following holography-critical parameters: spectral shift of sensitivity towards the long-wavelength region compared to the initial donor and acceptor components, as well as lower extinction coefficient of CTC ($\varepsilon = 10 - 10^3$ L·M^{-1}·cm^{-1}) [24] in contrast to the conventional sensitizer dyes ($\varepsilon \approx 10^4 - 10^5$ L·M^{-1}·cm^{-1}) [26], which is applicable in the homogeneous photopolymerization in thick layers [27]. Amine/phosphine-containing compounds are widely used as donor components, and iodonium/sulfonium salts are widely used as acceptors [24,28]. Under the influence of light, CTC is degraded with formation of an alkyl/aryl radical. It should be noted that the use of CTCs as initiators of holographic recording has been little studied.

PIS based on dye-co-initiator(s) are also widely used as sensitizers in the visible region of the spectrum [29–31]. One of the efficient co-initiators are the salts of (alkyl)(aryl)borates [32,33], and the mechanism of initiation of radical polymerization is explained in terms of a photoinduced electronic transition from the borate anion to the excited dye in a singlet or triplet state [34]. After electron transfer, alkyl triphenyl borate is disintegrated leading to formation of the alkyl radical $R'^{\bullet}$ and borane R_3B. Figure 1 shows a diagram of the mechanism that leads to the formation of an alkyl radical.

$$\text{Dye} \xrightarrow{h\psi} {}^{1,3}\text{Dye} \xrightarrow{R_3BR'^-} \text{Dye}^{-\bullet} + R_3B + R'^{\bullet} \rightarrow \text{Initiation}$$

Figure 1. Mechanism of alkyl radical initiation using borate salts as a co-initiator.

Note that the disadvantage of free radical photopolymerization is its inhibition by atmospheric oxygen in thin films [35]. The inhibition occurs due to the formation of peroxide radicals, which trap the free radicals and prevent further polymerization. A well-known approach to neutralizing the effect of oxygen inhibition of radical polymerization is the use of thiol-containing compounds in photopolymer compositions [36], which are not always compatible with other components of the compound. In this regard, the development of effective PIS without thiol-containing compounds capable of effective initiation of free radical polymerization under mild irradiation conditions (low light intensity and the possibility of polymerization in air) is still relevant [37,38]. Note that the use of such PIS will allow the holograms to be recorded in HPPM without any protective coatings on top of the recording layers, which introduce additional re-reflections of light and degrade the quality of the generated hologram.

Earlier in [39], we described a new charge transfer complex based on borate and sulfonium salts: butyltris(4-anisyl)2,4-diethyl-9-oxo-10-(4-heptyloxyphenyl)-9H-thioxanthenonium borate that absorbs in the entire visible range of the spectrum. This study was intended to develop and examine the spectral sensitivity of holographic photopolymer materials based on different PIS (HPPM-MB and HPPM-CTC, HPPM-MB-CTC) to laser radiation ($\lambda = 457,\ 532,\ 639$ nm), assess the diffraction efficiency of the reflecting holograms, as well as find the possibility of holograms formation in HPPM with a protection film preventing the oxygen ingress and without this film.

Experimental part

CTC-based HPPM

The basic compound of a photopolymer composition based on an acrylamide monomer and a polymer binder polyvinyl acetate was used in this paper [40]. As PIS we used a charge-transfer complex butyltris(4-anisyl)2,4-diethyl-9-oxo-10-(4-heptyloxyphenyl)-9H-thioxanthenonium borate ([S]-[B]), as well as a two-component photo-initiation system, the dye-co-initiator Methylene Blue / butyltris(4-anisyl)tetrabutylammonium borate ([Bu_4N][B]). For structural formulas of PIS, see Figure 2.

In spectra of initial PIS CTC components, 2,4-diethyl-9-oxo-10-(4-heptyloxyphenyl)-9H-thioxanthenium hexafluorophosphate ([S][PF_6]) and [Bu_4N][B] there's no any absorption in the visible part of the spectrum and when they mix, a bathochromic shift occurs in the absorption spectrum (Fig. 3).

The CTC-based compound was obtained by adding [S][PF_6] and [Bu_4N][B] into the chloroform solution of monomer and polymer matrix (c[S][PF_6] = [Bu_4N][B] = 40 wt% of monomer weight). If this concentration was exceeded, crystallization of the samples was observed. The concentration of MB in HPPM-MB was selected according to the guidelines in [41], where the optical density at the recording wavelength for reflection holograms should be within $D = 0.25 - 0.7$, the concentration of [Bu_4N][B] was 40 mass% of monomer weight. The holographic layers HPPM-CTC-MB were also obtained based on a combination of two PIS. Fig. 4 shows HPPM absorption spectra.

The thickness of dried photo-polymer layer of HPPM was $d_0 = 30 - 40\,\mu$m. After the solvent had been evaporated, a protective polyethylene terephthalate film was rolled onto the photopolymer layer, which prevented oxygen from entering the photosensitive layer. The thickness measurements of the samples were carried out using an upgraded interference microscope MII-4 [42].

Spectral signals of the recorded holograms were detected using a spectrometer (Avantes) right after irradiation of HPPM.

Recording and characterization of reflection holograms

The formation of monochrome and three-color holograms was carried out by sequential recording with laser radiation: in blue region (wavelength of $\lambda = 457$ nm), green ($\lambda = 532$ nm) and red ($\lambda = 639$ nm) regions. The holograms were recorded according to a scheme with two opposite rays, the angle of convergence of which was 110° (in the air) with a ratio of intensities in the detection plane 1 : 1. The period of formed gratings was ($p_{457} = 0.3$, $p_{532} = 0.35$, $p_{639} = 0.41\,\mu$m). Reflection holograms were recorded using a system described in detail in [43], the optical scheme of which is shown in Fig. 5.

The experimental values of diffraction efficiency (DE) of reflection holograms were estimated using the formula:

$$\eta_r = \left(1 - \frac{T_r}{T_0}\right) \times 100\%, \qquad (1)$$

where T_r — transmission values at wavelengths of the minimum of spectral profile and T_0 near its base [44,45]. Examples of the obtained spectral responses are shown below in Fig. 6.

The characterization of the obtained holograms included measuring the transmission spectrum of the reflection hologram using a digital spectrophotometer [46] directly during its recording, estimating the values of DE, modulating the refractive index and the degree of shrinkage of HPPM thickness. To calculate the kinetics of the formation of reflection holograms, transmission spectra were recorded

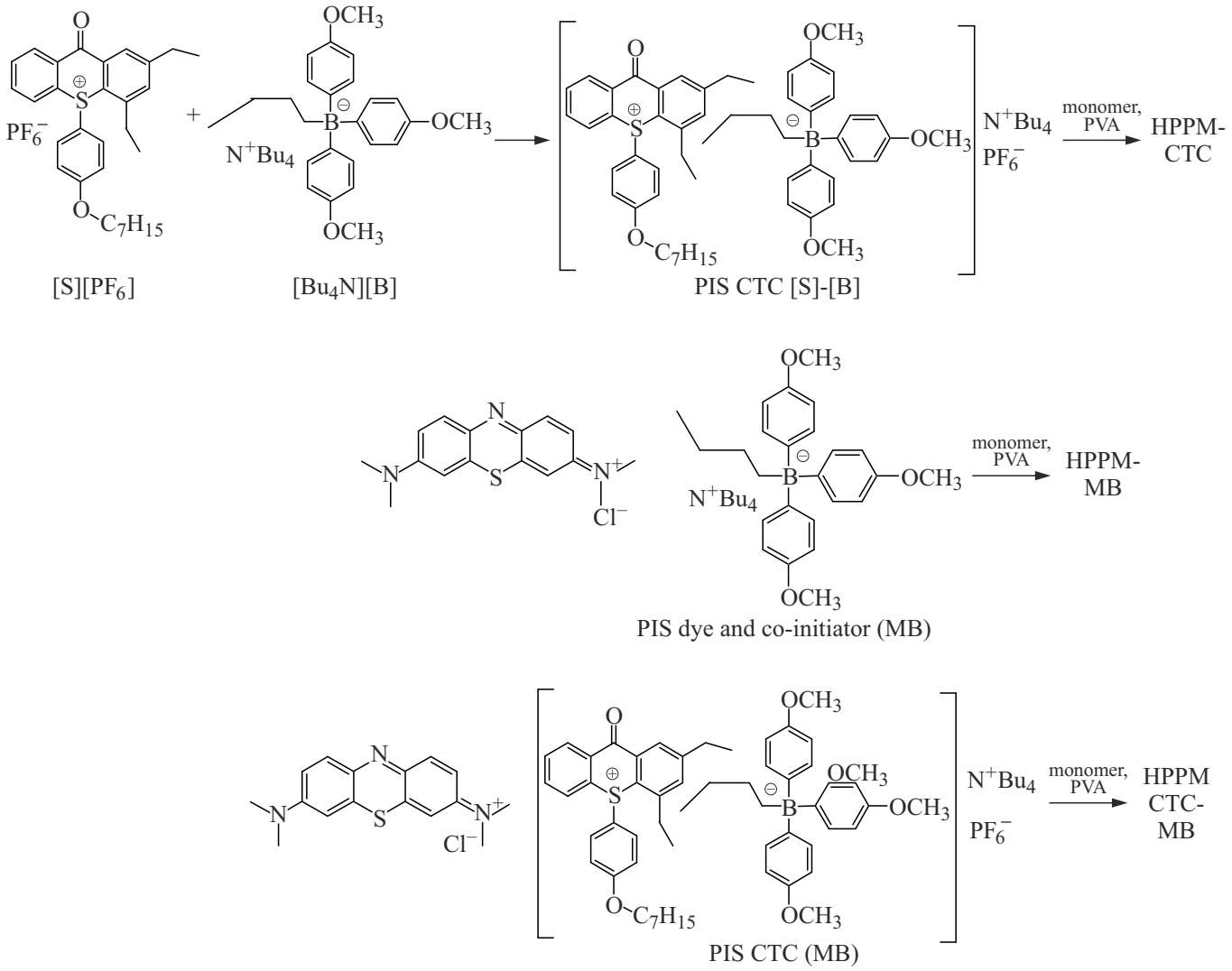

Figure 2. Structural formulas of PIS (CTC) and PIS (MB).

in real time on a spectrophotometer with a periodicity of 0.62 s. The kinetic curve is generated using software.

The calculated curves presented below are constructed taking into account Kogelnik's formulae [43,47]. The calculated data were obtained using a [48] software package to estimate the amplitude of the refractive index modulation and the nature of changes in the spatial structure of holographic gratings. The calculation was performed taking into account the absorption of the material.

Results and discussions

Formation of reflection holograms

From Fig. 3 and 4 we may see that CTC spectra in solution and HPPM layer have an absorption of up to 600−650 nm in contrast to initial components that absorb only up to 430 nm. The appearance of an additional absorption arm is associated with formation of CTC [S]−[B]. The large bathochromic shift of CTC absorption spectrum compared to the original components makes it possible to record color holograms using laser radiation with wavelengths located in the entire visible range (400−650 nm). In HPM film, CTC absorption is similar, but there is a difference in the optical density values. Thus, in chloroform, the optical density of CTC in 425−475 nm region lies in the range of $D \approx 0.4 - 0.45$, and in the polyvinyl acetate film $D \approx 0.05 - 0.1$, which is due to the different thickness of the absorbing substance. It should be noted that the solvent can affect the spectral properties of CTC, as well as the stability of complex compounds [49].

According to Fig. 4, in the absorption spectrum of HPPM with a photo-initiation system, the dye/co-initiator is Methylene Blue/butyltris(4-anisyl)tetrabutylammonium borate contains the main absorption peak of the dye in the red visible spectrum with a maximum of 670 nm and a weak

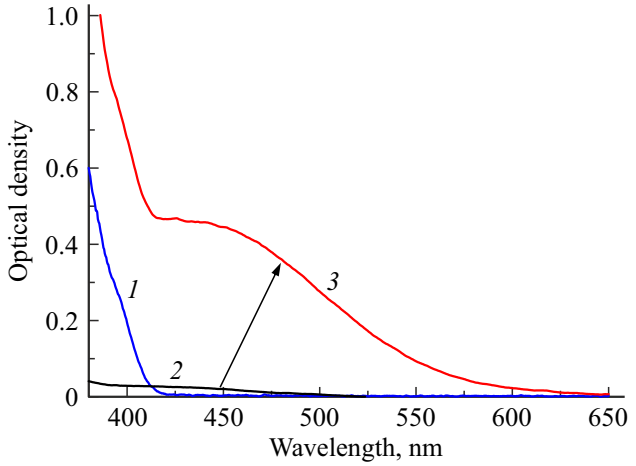

Figure 3. UF-visible absorption spectra S][PF6] (*1*), [Bu4N][B] (*2*) and CTC [S]–[B] on their basis (*3*). (c[S][PF6] = c[Bu4N][B] = $2.5 \cdot 10^{-6}$ mol/L) 1.5 mg in 1 ml $CHCl_3$. Length of optical path is 1 cm.

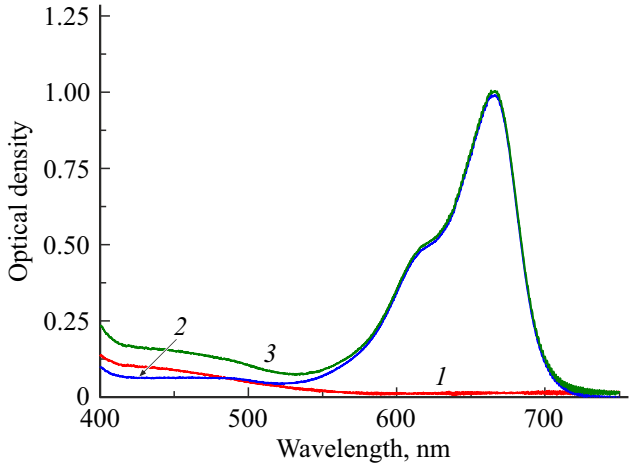

Figure 4. UF-visible absorption spectra HPPM-CTC (*1*), HPPM-MB (*2*) and combined HPPM-CTC-MB (*3*).

absorption band in the region of 440–540 nm. The optical density in the area of the absorption band is close to that of HPMC TC, which makes it possible to record and compare holograms in this area for both types of PIS under similar conditions of the initial absorption of the photolayer.

It can also be seen from Fig. 4 that the combination of the two PISs made it possible to increase the optical density in the blue-green region of the visible spectrum to $D = 0.1 - 0.17$.

Figure 6 shows the transmission spectra of reflection holograms (reflexes) obtained on photopolymer films HPPM-CTC, HPPM-MB, HPPM-CTC-MB exposed to irradiation by lasers with the wavelengths of 457, 532 and 639 nm. Fig. 6, β-c shows superimposed spectra of recorded monochrome holograms (in different regions of HPM). Figure 6, *d* shows the spectrum of a three-color hologram formed by parallel (simultaneous) recording with three lasers).

The spectral shift of the hologram reflections observed in the above graphs relative to the laser radiation wavelength is associated with the difference in the angle of convergence of the beams during hologram recording and the incidence angle of the probing beam, as well as the effect of shrinkage of the hologram thickness ($\approx 2 - 3\%$) due to photopolymerization. Summary data on the characteristics of the recorded reflection holograms are given in the table.

The table shows that the maximum achievable diffraction efficiency, refractive index modulation, and spectral sensitivity of hologram recording in case of CTC-based HPPM decrease as the recording wavelength rises from $DE_{457} \approx 84\%$ ($E_{457} = 76\,\text{mJ/cm}^2$) to $DE_{532} = 57\%$ ($E_{532} = 105\,\text{mJ/cm}^2$). When the holograms were recorded by red laser $DE_{639} \approx 21\%$ was observed, at that, the recording energy was the lowest ($E_{639} = 223\,\text{mJ/cm}^2$), which is due to decreased optical density of HPPM-CTC from $D_{457} \approx 0.1$ to $D_{639} = 0.01$ and, as a consequence, low absorbed energy.

It is noteworthy that on HPPM-MB, when irradiated with a red laser $\lambda = 639$ nm, in the region of which MB has the main absorption ($D = 0.62$), $DE \approx 72\%$ was obtained, while the recording energy was $E_{639} = 18\,\text{mJ/cm}^2$.

Weak absorption in HPPM-MB in the blue-green region ($D_{457} = 0.06$ $D_{532} = 0.05$) allowed to record holograms using lasers with the wavelength of $\lambda = 457$ and 532 nm with DE over 40%, however, to reach maximal DE it was required to increase the recording energy to $50\,\text{mJ/cm}^2$.

It is known that in HPPM, due to radiation absorption, hologram recording is uneven in thickness, and therefore the concept of the effective thickness of the formed hologram (d_{ef}) is introduced, which can be estimated by the formula [41,50]

$$d_{ef} = d_0 \exp\left(-\frac{D}{2}\right), \qquad (2)$$

where d_0 — physical thickness of HPPM, D — optical density of hologram at the recording wavelength.

In table we may see the values of the hologram effective thickness. The effective thickness turns out to be different for the studied HPPM-CTC and HPPM-MB at the specified wavelengths due to differences in the optimal values D. In particular, with the increase of laser radiation wavelength in HPPM-CTC we may see increase $d_{ef457} = 29\,\mu$m to $d_{ef639} = 33\,\mu$m, while at the same time for HPPM-MB the effective thickness decreased from $d_{ef457} = 35\,\mu$m to $d_{ef639} = 30\,\mu$m.

It can be seen from the data obtained that as the recording wavelength increases, the sensitivity of HPPM CTC and the diffraction efficiency of the generated holograms go down. At the same time, HPPM-MB has a high sensitivity in the red region of the spectrum, which predetermined the combining of PIS and creating hboxHPPM-MB-CTC. From the table above we may see that by uniting two PIS in HPPM-MB-CTC we managed to slightly raise the

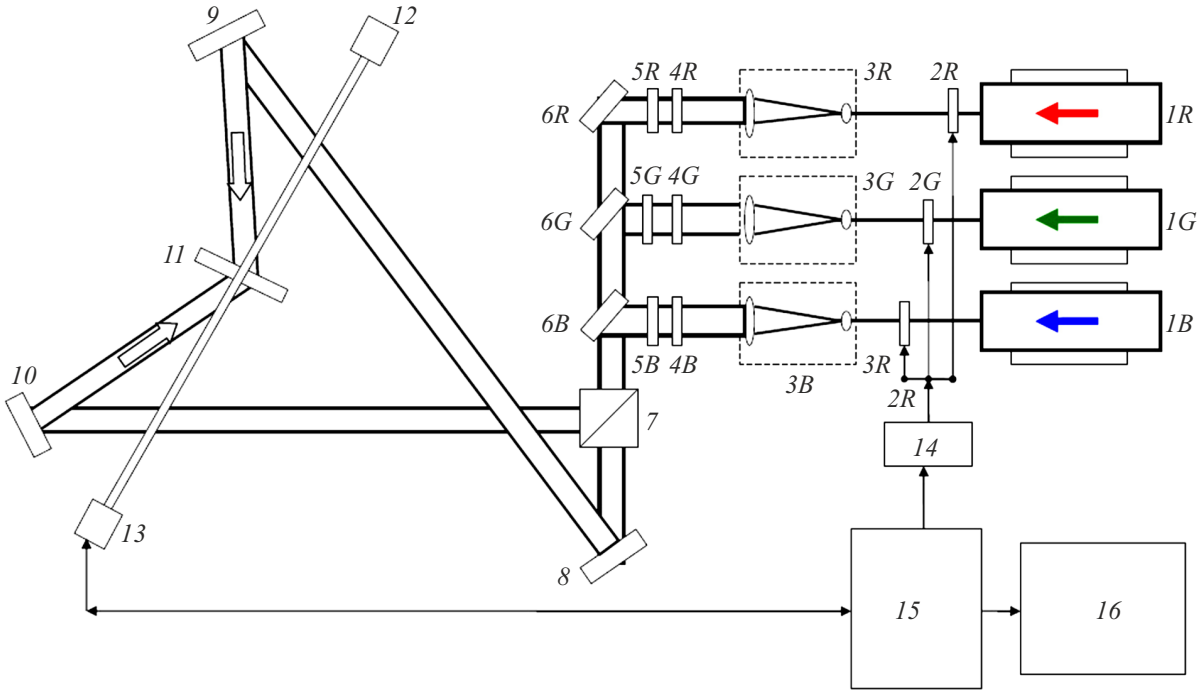

Figure 5. System for recording color volume reflection holograms. *1* — lasers; *2* — automated photographic shutter; *3* — collimators; *4* — diaphragms; *5* — neutral light filters; *6* — dichroic mirrors; *7* — beam splitter cube; *8, 9, 10* — flat mirrors *11* — HPPM sample; *12* — halogen lamp to form the white probing light beam; *13* — digital spectrophotometer; *14* — shutters control unit; *15* — computer; *16* — monitor. Indices *b, g, r* relate to „blue“ (457 nm), „green“ (532 nm) and „red“ (639 nm) channels, respectively.

Characteristics of HPPM and recorded reflective holograms based on them

		λ_{rec}, nm	D (Optical density)	d_{ef}, μm	P, mW/cm^2	E, mJ/cm^2	DE, %	Δn (refractive index modulation)
HPPM-CTC	Monochrome holograms	457	0.09	29	3.8	76	84	0.0077
		532	0.02	31	3.5	105	57	0.006
		639	0.01	33	9	223	21	0.0031
HPPM-MB	Monochrome holograms	457	0.06	35	3.8	45	43	0.0037
		532	0.05	36	3.5	50	54	0.0051
		639	0.62	30	1	18	72	0.01
HPPM-CTC-MB	Monochrome holograms	457	0.15	30	3.8	38	47	0.005
		532	0.07	28	3.5	45	48	0.0067
		639	0.63	30	1	17	72	0.0097
HPPM-CTC-MB	Parallel recording, three-color holograms	457	0.15	25	3.8	19	39	0.0051
		532	0.07	27	3.5	17	41	0.0058
		639	0.63	27	1	5	21	0.0042

photo-polymers efficiency in the blue region of visible spectrum ($E_{457} = 38$ mJ/cm^2) compared to HPPM-MB ($E_{457} = 45$ mJ/cm^2), which is explained by higher optical density of HPPM in the blue-green region from 0.06 to 0.15.

It is noteworthy that in the hologram absorption spectrum profile obtained on HPPM-CTC-MB at a wavelength of 639 nm, side lobes are visible, which can be explained by the formation of a more uniform spatial structure of the hologram grating.

Figure 6, *d* shows the transmission spectrum of a three-color hologram formed in HPPM-CTC-MB in parallel recording mode. Holograms with a close degree of spectral

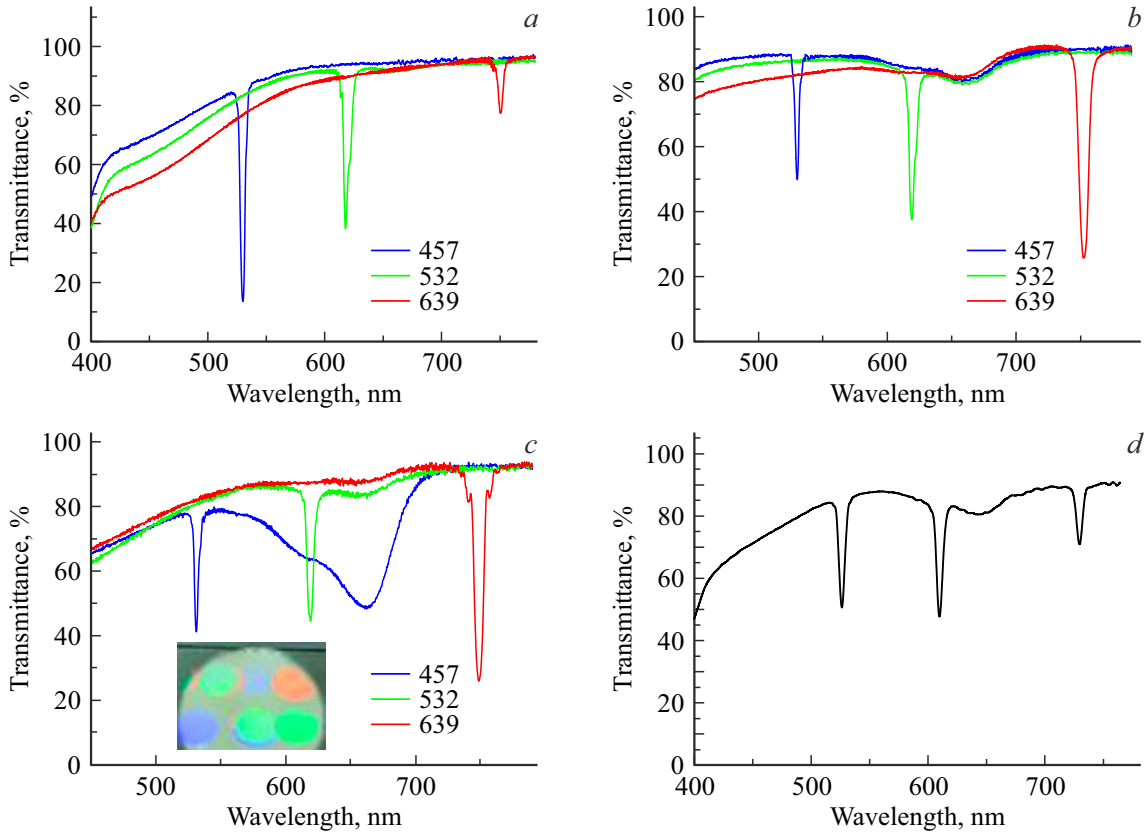

Figure 6. Experimental graphs of transmission spectra of reflection color holograms (λ_{rec} = 639, 532, 457 nm) with HPPM thicknesses of $d_0 = 25 - 30\,\mu$m: (*a*) HPPM-CTC; (*b*) HPPM-MB; (*c*) HPPM-CTC-MB in the mode of sequential recording, the insert window shows the appearance of holograms when irradiated by white light; (*d*) HPPM-CTC-MB in the mode of parallel recording.

responses were created by simultaneous irradiation with three lasers with optimized power density to form spectral responses with a close value of diffraction efficiency (see the Table). Eventually, a three-color hologram war recorded having $DE_{457} \approx 39\%$, $DE_{532} \approx 41\%$, $DE_{639} \approx 21\%$, with total refraction index modulation amounting to ≈ 0.015.

It should be noted that such characteristics of the developed holograms as shrinkage, spectral sensitivity range, sensitivity value are close to commercially available photopolymers, which are widely used to create color holograms [51].

Kinetics of reflection hologram formation

Figure 7 shows kinetic curves of recording the reflection holograms in MB- and CTC-based HPPM. The samples had the same optical density at the recording wavelength of $D_{457} = 0.05$.

Fig. 7 shows that HPPM-CTC has a lower reactivity compared to HPPM-MB. The induction period was increased from 0.6 to 1.2 s for HPPM-CTC, and the curve saturation is observed for HPPM-CTC during 5 s, after which a small growth of *DE* from 45 to 50% occurs during 5 s. The kinetic saturation curve for HPPM-MB is observed for 4 s, after which further growth stops. So, we can conclude that an increase in the recording power density made it possible to initiate radical polymerization in HPPM-MB more efficiently than in samples of HPPM-CTC.

Prevention of oxygen inhibition in HPPM-CTC, HPPM-MB

To identify the possibility of preventing oxygen inhibition in thin layers of HPPM-MB and HPPM-CTC, we detected the kinetics of reflection holograms recording in HPPM without protective films preventing oxygen ingress (Fig. 7).

It can be seen that the holograms recorded on HPPM-MB and HPPM-CTC, both with and without protective film preventing oxygen ingress, have similar kinetic curves (Fig. 7). The induction period for HPPM didn't exceed 1 s. HPPM-CTC spectra with a protective film applied have a higher initial rate of change in the refractive index modulation than without this film. For HPPM-MB the rates of hologram recording are similar. After reaching saturation, the formed holograms had a close value of the refractive index modulation of materials $\Delta n \approx 0.008$. Thus, the use of borate salt both as a donor component in PIS-CTC and as a co-initiator with MB effectively prevents oxygen inhibition of radical polymerization and allows holographic recording without protective coatings of recording layers.

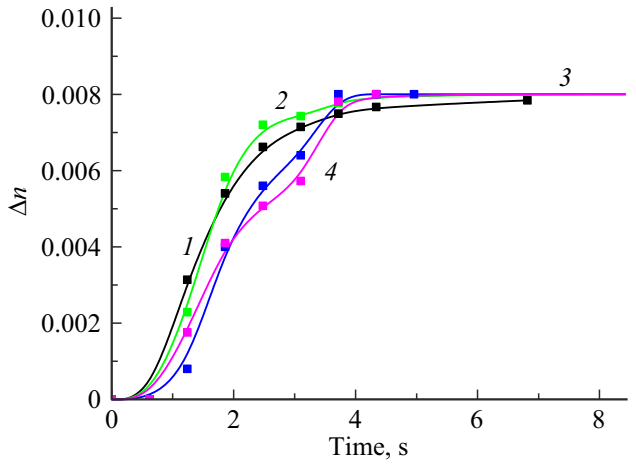

Figure 7. Kinetic curves of the change in the refractive index modulation of materials with and without a protective film when recording the reflection holograms ($\lambda_{rec} = 457$ nm, $I = 29\,\text{mW}\cdot\text{cm}^{-2}$): HPPM-MB ($D = 0.03$) (*1, 2*), HPPM-CTC ($D = 0.1$) (*3, 4*) with ingress (*1, 3*) and without ingress (*2, 4*) of oxygen.

Conclusion

Holographic photopolymer materials have been developed using new photo-initiating systems based on a photosensitive charge transfer complex: butyltris(4-anisyl)diethyl-9-oxo-10-(4-heptyloxyphenyl)-9H-thioxanthenonium borate and Methylene Blue photo-initiation systems: butyltris(4-anisyl)tetrabutylammonium borate. The spectral characteristics of CTC in solution and polymer matrix have been studied, and the holographic characteristics of HPPM have been compared with those of various PIS in sequential and parallel recording of color holograms.

It was demonstrated that PIS are featuring sensitivity in a wide spectral range. Through combining two PIS it became possible to increase the sensitivity of HPPM in the blue region from 45 mJ/cm^2 to 38 mJ/cm^2.

Monochrome reflection holograms were formed using laser radiation with wavelengths of 457, 532, and 639 nm. Using parallel recording with three lasers, a three-color hologram was formed in HPPM-CTC-MB with $DE_{457nm} \approx 40\%$, $DE_{532nm} \approx 43\%$, $DE_{639nm} \approx 19\%$.

It was revealed that the use of PIS based on butyltris(4-anisyl) borate makes it possible to effectively prevent oxygen inhibition allowing to record the reflection holograms without using protective films on top of the recording layer.

Acknowledgments

The authors would like to thank the Chemical Research Center of Collective Use of Siberian Branch of the Russian Academy of Sciences for their assistance in performing spectral and analytical measurements.

Funding

This study was financially supported by the Organic Chemistry Research and Scientific Institute of SB RAS № 075-00365-25-00 and within the project of the Fundamental Scientific Research of the state science academies for 2021-2025 No. 0238-2021-0006 and S&R study „Highly informative optical methods for studying the composition and microstructure of materials and substances: physical fundamentals, methods of implementation and use“ № 124041700108-6 (FWNG-2024-0022).

Conflict of interest

The authors declare that they have no conflict of interest.

References

[1] G.S. Zheng, Y. Jiang, T. Wang, Huang A., Y. Zhang, P. Tang, S. Zhuang, Y. Liu, S. Yin. Opt. Express, **19** (3), 2216 (2011). DOI: 10.1364/OE.19.002216
[2] J. Guo, M.R. Gleeson, J.T. Sheridan. Physics Research International, **1**, 2090 (2012). DOI: 10.1155/2012/803439
[3] A. Zanutta, E. Orselli, T. Facke, A. Bianco. Optical Materials Express, **6** (1), 252 (2016). DOI: 10.1364/OME.6.000252
[4] N. Vorzobova, P. Sokolov. Polymers, **11** (12), 2020 (2019). DOI: 10.3390/polym11122020
[5] Holoexpo. Nauka i praktika [Electronic resource] (in Russian). URL: http://www.holoexpo.ru
[6] W.S. Colburn, K.A. Haines. Applied Optics, **10** (7), 1636 (1971).
[7] V. Mikerin, V. Ugozhaev. J. Opt. Technol., **9** (4), 213 (2023). DOI: 10.1364/JOT.90.000213
[8] J. Li, P. Hu, Z. Zeng, J. Jin, J. Wu, X. Chen, J. Liu, Q. Li, M. Chen, Z. Zhang. Molecules, **27** (19), 6283 (2022). DOI: 10.3390/molecules27196283.
[9] M.D. Alim., D.J. Glugla, S. Mavila, C. Wang, P.D. Nystrom, A.C. Sullivan, C.N. Bowman. ACS Applied Materials & Interfaces, **10** (1), 1217 (2017). DOI: 10.1021/acsami.7b15063
[10] F.K. Bruder, T. Facke, T. Rolle. Polymers, **9** (12), 472 (2017). DOI: 10.3390/polym9100472
[11] D. Cody, S. Gul, T. Mikulchyk, M. Irfan, A. Kharchenko, Goldyn, S. Martin, S. Mintova, J. Cassidy, I. Naydenova. Appl. Opt., **57**, 173 (2018). DOI: 10.3390/polym11122020
[12] D.A. Belousov, R.I. Kuts, K.A. Okotrub, V.P. Korolkov. Photonics, **10** (7), 771 (2023). DOI: 10.3390/photonics10070771
[13] B. Guo, M. Wang, D. Zhang, M. Sun, Y. Bi, Y. Zhao. ACS Applied Materials & Interfaces, **15** (20), 24827 (2023). DOI: 10.1021/acsami.3c01446
[14] A. Ibrahim, X. Allonas, C. Ley, K. Kawamura, H. Berneth, F.K. Bruder, T. Facke, R. Hagen, D. Honel, T. Rolle, G. Walze, M.S. Weiser. Chemistry — A European Journal, **20** (46), 15102 (2014). DOI: 10.1002/chem.201404072
[15] E.M. Mihaylova. Coatings, **12** (11), 1765 (2022). DOI: 10.3390/coatings12111765
[16] D. Zhang, Y. Zhao, B. Guo, Z. Zhang, D. Hu, Z. Wang, J. Zhu, Y. Ye, Y. Zhao. European Polymer Journal, **198**, 112436 (2023). DOI: 10.3390/polym15132908

[17] A. Ibrahim, X. Allona, C. Ley, B.E. Fouhaili, C. Carre. J. Photopolymer Science and Technology, **27** (1), 517 (2014). DOI: 10.1021/cm402262g
[18] G. Ding, C. Jing, X. Qin, Y. Gong, X. Zhang, S. Zhang, Z. Luo, H. Li, F. Gao. Dyes Pigm., **137**, 456 (2020). DOI: 10.1016/j.dyepig.2016.10.034
[19] W. Liao, C. Xu, X. Wu, Q. Liao, Y. Xiong, Z. Li, H. Tang. Dyes Pigm., **178**, 108350 (2020). DOI: 10.1016/j.dyepig.2020.108350
[20] A. Ibrahim, C. Ley, X. Allonas, C. Carre, I. Pillin. J. Displ. Technol., **10**, 456 (2014). DOI: 10.1109/JDT.2014.2314863
[21] J. Kabatc, K. Iwinska, A. Balcerak, D. Kwiatkowska, A. Skotnicka, Z. Czech, M. Bartkowiak. RSC Advances, **10** (42), 24817 (2020). DOI: /10.1039/D0RA03818K
[22] C. Forster, A. Andrieu-Brunsen. Chem. Commun., **59** (12), 1554 (2023). DOI: 10.1039/D2CC06595A
[23] K. Kawamura, H. Berneth, F. K. Bruder, T. Facke, R. Hagen, D. Honel, T. Rolle, G. Walze, M.S. Weiser. Chemistry — A European J., **20** (46), 15102 (2014). DOI: 10.1002/chem.201404072
[24] D. Derevyanko, V. Shelkovnikov, V. Kovalskii, I. Zilberberg, S. Aliev, N. Orlova, V. Ugozhaev. Chemistry Select, **5** (38), 11939 (2020). DOI: 10.1002/slct.202002163
[25] Q. Ma, L. Buchon, V. Magné, B. Graff, F. Morlet-Savary, Y. Xu, M. Benltifa, S. Lakhdar, J. Lalevée. Macromolecular rapid commun., **43** (19), 2200314 (2020). DOI: 10.1002/marc.202200314
[26] I.Y. Kargapolova, N.A. Orlova, K.D. Erin, V.V. Shelkovnikov. Russian J. Organic Chemistry, **52**, 37 (2016). DOI: 10.1134/S1070428016010073
[27] P. Garra, B. Graff, F. Morlet-Savary, C. Dietlin, J.-M. Becht, J.-P. Fouassier, J. Lalevée. Macromolecules, **51** (1), 57 (2018). DOI: 10.1021/acs.macromol.7b02185
[28] D. Wang, P. Garra, S. Lakhdar, B. Graff, J. Fouassier, H. Mokbel, M. Abdallah, J. Lalevée. ACS Appl. Polym. Mater., **1** (3), 561 (2019). DOI: 10.1021/acsapm.8b00244
[29] V.V. Shelkovnikov, E.V. Vasil'ev, V.V. Russkikh. Optoelectronics, Instrumentation and Data Processing, **52**, 404 (2016). DOI: 10.3103/S8756699016040130
[30] F. Dumur. Catalysts, **13**, 493 (2023). DOI: 10.3390/catal13030493.
[31] C.Y. Shih, J.-S. Ni, Y.-C. Chen. Macromolecular Chemistry and Physics, **1** (2024). DOI: 10.1002/macp.202300428
[32] G.C. Weed, B.M. Monroe. United States Patent 5143818. Borate coinitiators for photopolymerizable compositions (1992).
[33] J. Kabatc, K. Iwińska, A. Balcerak, D. Kwiatkowska, A. Skotnicka, Z. Czech, M. Bartkowiak. SC Advances., **10**, 24817 (2020). DOI: 10.1039/D0RA03818K
[34] X. Allonas, A. Ibrahim, C. Ley, H. Saimi, J. Bugnet, K. Kawamura. J. Photopolymer Science and Technology, **24** (5), 531 (2011). DOI: 10.2494/photopolymer.24.531
[35] N. Li, X.-C. Pan. Chinese J. Polymer Science, **39**, 1084 (2021). DOI: 10.1007/s10118-021-2597-9
[36] V.V. Shelkovnikov, D.I. Derevyanko, L.V. Ektova. Polymer Science, Series B, **58** (5), 519 (2016). DOI: 10.1134/S1560090416050109
[37] S. Ke, X. Pu, D. Frederic, L. Jacques. J. Polymer Science, **59** (13), 1338 (2021). DOI: 10.1002/pol.20210225
[38] F. Dumur. European Polymer J., **195**, 112193 (2023). DOI: 10.1016/j.eurpolymj.2023.112193
[39] D.I. Derevyanko, E.F. Pen., V.V. Shelkovnikov, V.V. Bardin. In vol.: *HOLOEXPO 2022, Theses of reports. XIX Mezhdunarodnaya konferentsiya po gologrаfii i prikladnym opticheskim tekhnologiyam* (St.Petersburg, 2022), p. 322–329.
[40] C. Choi, E.V. Vasiliev, V.V. Shelkovnikov, V. Loskutov. Patent US9874811B2 Photopolymer composition for holographic recording (2016).
[41] V.V. Shelkovnikov, E.F. Pen, V.I. Kovalevsky. Optical Memory and Neural Networks, **16**, 75 (2007). DOI: 10.3103/S1060992X07020038
[42] V.P. Korol'kov, A.E. Kachkin, R.V. Shymanskiy. Mir izmereniy, **10**, 37 (2012) (in Russian).
[43] D.I. Derevyanko, E.F. Pen, V.V. Shelkovnikov, S.I. Aliev. Optoelectronics, Instrumentation and Data Processing, **57** (6), 584 (2021). DOI: 10.3103/S8756699021060042
[44] W.K. Smothers et al. Dry film process for altering wavelength response of holograms. US Patent 5024909. 1991. https://www.freepatentsonline.com/5024909.pdf
[45] V.V. Shelkovnikov, E.V. Vasiliev, V.V. Russkikh. Avtometriya. **52** (4), (in Russian). 107 (2016). DOI: 10.15372/AUT20160413
[46] S.A. Babin, E.V. Vasiliev, V.I. Kovalevskiy, E.F. Pen, A.I. Plekhanov, V.V. Shelkovnikov. Avtometrija., **39** (2), 57 (2003) (in Russian).
[47] H. Kogelnik. The Bell System Technical J., **48**, 2909 (1969).
[48] E.F. Pen, M.Y. Rodionov, V.V. Shelkovnikov. J. Optical Technology, **73** (7), 475 (2006). DOI: 10.1364/JOT.73.000475
[49] S.V. Dushina, V.A. Sharnin. Khimiya i khimicheskaya tekhnologiya, **56**, (in Russian). 3 (2013).
[50] S.H. Stevenson, K.W. Steijn. Proc. SPIE, **2405**, 88 (1995). DOI: 10.1117/12.205352
[51] I. Vazquez-Martín, M. Gomez-Climente, J. Marin-Saez, M.V. Collados, J. Atencia. Proc. SPIE., **10233**, 64 (2017). DOI: 10.1117/12.2265802

Translated by T.Zorina